Available online at www.sciencedirect.com
SCIENCE DIRECT
Talanta 67 (2005) 1029–1034
Talanta
www.elsevier.com/locate/talanta

Fluorescence resonance energy transfer in doubly-quantum dot labeled IgG system

Qiang Ma [a], Xing-Guang Su [a,*], Xin-Yan Wang [a], Yi Wan [a], Chun-Lei Wang [b], Bai Yang [b], Qin-Han Jin [a]

[a] *Institute for Miniature Analytical Instrumentation, College of Chemistry, Jilin University, Changchun 130023, PR China*
[b] *Key Lab for Supramolecular Structure and Materials, College of Chemistry, Jilin University, Changchun 130023, PR China*

Received 12 January 2005; received in revised form 21 April 2005; accepted 21 April 2005
Available online 31 May 2005

Abstract

The mouse immunoglobulin G (mouse IgG) as a kind of bio-molecule was labeled with two different luminescent colloidal semiconductor quantum dots (QDs), green-emitting CdTe quantum dots and red-emitting CdTe quantum dots in this work. As a result of the fluorescence resonance energy transfer (FRET) between the two different sizes nanoparticles with mouse IgG as the binding bridge, a significant enhancement of the emission of the red-emitting CdTe quantum dots and the corresponding quenching of the emission of green-emitting CdTe quantum dots were observed. The relationship between the concentration of the mouse immunoglobulin G and the fluorescence intensity ratio (I_a/I_d) of acceptors and donors was studied also. Under optimal conditions, the calibration graph is linear over the range of 0.1–20.0 mg/L mouse IgG.

Keywords: Quantum dots; Fluorescence resonance energy transfer; Immunoglobulin G

1. Introduction

The quantitative determination of protein is very important and essential in clinical medicine, biochemistry and laboratory practice. But the conventional methods have some limitation in terms of sensitivity, selectivity, stability and simplicity, such as the Lowry assay [1], the Bradford method [2], the bromophenol blue [3,4] and bromocresol green procedures [5]. In recent years, several groups have shown that surface ligands can be used to attach various biological molecules to form QD-bioconjugates [6–13]. As an alternative to conventional fluorophores, QDs offer a number of attractive features, including high photo-bleaching threshold, good chemical stability, relatively narrow and symmetric luminescence bands, readily tunable spectral properties and a relatively large detectable optical signal. These QDs can be detected at concentrations comparable to the best conventional organic dyes by conventional fluorescence spectrometers, and individual bioconjugated QDs are observable by confocal microscopy [8]. These properties combined make these materials attractive for labeling with functional biomolecules for fluorescent tagging applications. Colloidal QDs are approximately spherical nanocrystals with surfaces that can be derived with a variety of functional capping groups (surface ligands), allowing their dispersion in a range of solvents, including aqueous environments [6–8,13]. The surface ligands can be used to attach biomolecules to form QD-bioconjugates. The water-compatible CdTe QDs having carboxylic acid terminal groups linked with biomolecule for QD-bioconjugate formation where conjugation is driven by electrostatic self-assembly have been elaborated [6–8].

Fluorescence resonance energy transfer (FRET) occurs when the electronic excitation energy of a donor chromophore is transferred to an acceptor molecule nearby via a through-space dipole–dipole interaction between the donor–acceptor pair [14–18]. The FRET process is more efficient when there is an appreciable overlap between the emission spectrum of the donor and the absorption spectrum

* Corresponding author. Tel.: +86 431 8499976; fax: +86 431 8499805.
E-mail address: suxg@mail.jlu.edu.cn (X.-G. Su).

0039-9140/$ – see front matter © 2005 Elsevier B.V. All rights reserved.
doi:10.1016/j.talanta.2005.04.036

of the acceptor [15–18]. The strong distance dependence of the FRET efficiency has been widely exploited in studying the structure and dynamics of proteins and nucleic acids, in the detection and visualization of intermolecular association, and in the development of intermolecular binding assays [19]. Compared with conventional chemical analysis, FRET-based analytical method has higher sensitivity and more simplicity in detection of ligand–receptor binding by observing merely the enhanced fluorescence of the acceptor.

FRET-based studies involving pairs of organic dye molecules as the donor–acceptor complexes are often limited by cross-talk caused by spectral overlap of the donor and acceptor emission. Several recent reports have confirmed that QDs, such as CdSe and CdTe, are able to participate in resonance energy transfer processes analogous to FRET, which overcome some of the limitations associated with conventional organic dye molecules in FRET-based studies of biomolecules with their features as mentioned before [12,18–21].

Our recent work has focused on fluorescence quenching effects in $QDs_{(G)}$/immunoglobulin G/$QDs_{(R)}$ assemblies where the immunoglobulin G had been labeled with QDs of two different sizes. Results got with solution phase showed that the excited-state dipole–dipole coupling between QDs of different sizes results in an excitation energy transfer from QDs of smaller diameters (green-emitting) to those with larger diameters (red-emitting), i.e., fluorescence resonance energy transfer. The FRET process between CdTe QDs of two sizes was confirmed by the changes of their spectra. The FRET efficiency (E) and the Stern–Volmer quench constant (K_{sv}) were calculated. Moreover, the influences of ionic strength, pH and the varying concentration of mouse immunoglobulin G on the FRET process were studied in some detail. Specifically, we employ one size of QDs linked with another size of QDs-labeled biological receptors that utilize donor–acceptor energy transfer between QDs for conducting recognition-based assays.

2. Experimental

2.1. Instrumentation

Fluorescence experiments were performed on a Shimadzu RF-5301 PC spectrofluorophotometer. UV–vis absorption spectra were obtained using a Varian GBC Cintra 10e UV–vis spectrometer. In either experiment a 1 cm path length quartz cuvette was used to measure the absorption or fluorescence spectrum. All optical measurements were carried out at room temperature under ambient conditions. All pH measurements were made with a PHS-3C pH meter (Hangzhou, China).

2.2. Chemicals and materials

All chemicals used were of analytical reagent grade without further purification. 3-Mercaptopropyl acid (MPA) (99+ %), tellurium powder (~200 mesh, 99.8%), $CdCl_2$ (99+ %), $NaBH_4$ (99%) were purchased from Aldrich Chemical Co. Mouse immunoglobulin G (mouse-IgG, 10 mg) was purchased from Beijing Dingguo Biotechnology Ltd., China, and used without further purification. The antigen powder was dissolved in a 2 mmol/L phosphate buffered saline solution (PBS, pH 7.3) to obtain 1 mg/mL solution and stored at 0–4 °C, dilute only prior to immediate use. Water used throughout was doubly distilled water (>18 MΩ cm).

2.3. Preparation of water-compatible CdTe quantum dots

Stable water-compatible CdTe quantum dots were prepared by deriving nanocrystal surfaces with MPA as described in previous papers [22,23]. In brief, sodium hydrogen telluride (NaHTe) was produced in an aqueous solution by reaction of sodium borohydride ($NaBH_4$) with tellurium powder at a molar ratio of 2:1 at first. Later, freshly synthesized oxygen-free NaHTe solution was mixed with nitrogen-saturated 1.25×10^{-3} mol/L $CdCl_2$ aqueous solution at pH 11.4, with MPA as a stabilizing agent. The molar ratio of Cd^{2+}:MPA:HTe^- was fixed at 1:2.4:0.5. The resulting mixture was then subjected to refluxing to control the size of the CdTe nanocrystals. Finally the QDs of different sizes were synthesized under different refluxing conditions separately. The final nanocrystal dispersions are stable in basic aqueous solutions (pH > 6). As the quantity of Cd^{2+} was excessive (from the molar ratio of Cd^{2+} and HTe^-) in reaction mixture, the concentration of CdTe QDs was calculated through the quantity of HTe^-. A luminescence quantum yield of ~25% was measured for the CdTe nanoparticles at room temperature by comparing with the fluorescence emission of Rhodamine 6G [24]. Two different QDs with emission maximum at 535 nm (green-emitting), 590 nm (red-emitting), respectively, were used in the present study (Fig. 1)

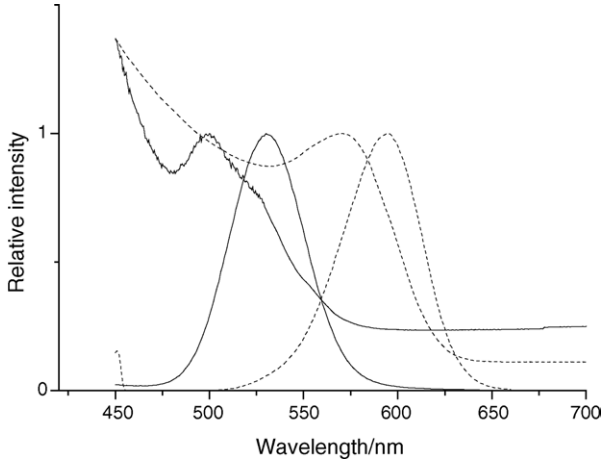

Fig. 1. Normalized absorption and emission spectra obtained from solutions of CdTe $QDs_{(G)}$ (solid) and $QDs_{(R)}$ (dashed). Solutions were prepared in 2 mmol/L PBS buffer (pH 7.3).

2.4. Bioconjugation of QDs with immunoglobulin G

Bioconjugation of immunoglobulin G with two sizes of MPA capped CdTe QDs was carried out by mixing the mouse immunoglobulin G (IgG) and $QDs_{(G)}$ (smaller diameters, green-emitting) in 1 ml of 2 mmol/L PBS buffer solution (pH 7.3) and then incubated for approximately 1 h at room temperature first. Then the $QDs_{(R)}$ (larger diameters, red-emitting) were added to the complex. The resulting solution contained stable $QDs_{(G)}$-IgG-$QDs_{(R)}$ conjugation without obvious aggregates was ready for assay. The emission spectra of the bioconjugate solutions were measured by using a RF-5301 PC fluorometer with excitation wavelength at 342 nm.

3. Results and discussion

3.1. Fluorescence and absorption spectra

The absorption and emission spectra obtained from two sizes of free CdTe quantum dots $QDs_{(G)}$ and $QDs_{(R)}$ in PBS buffer solution (pH 7.3) were shown in Fig. 1. The right QDs sizes were chosen in order to maximize the spectral overlap of the donor–acceptor emission and absorption spectra while still maintaining good spectral resolution of the donor and acceptor emission. The maximal emission peak of the $QDs_{(G)}$ is at 535 nm, while that of the $QDs_{(R)}$ is at 590 nm. So there is appreciable overlap between the emission spectrum of the $QDs_{(G)}$ (donor) and the absorption spectrum of the $QDs_{(R)}$ (acceptor).

3.2. Fluorescence spectra of $QDs_{(G)}$–IgG–$QDs_{(R)}$ system

The fluorescence spectra change obviously when $QDs_{(R)}$ conjugate with mouse immunoglobulin G which has been labeled with $QDs_{(G)}$, as shown in Fig. 2.

The effect of buffer pH and ionic strength on the conjugation between CdTe quantum dots and mouse immunoglobulin G were investigated, respectively.

3.2.1. Effect of the buffer pH

The effect of the buffer pH on the fluorescence spectra of the $QDs_{(G)}$–IgG–$QDs_{(R)}$ system was studied. The fluorescence intensity of $QDs_{(G)}$ at 535 nm increased gradually along with the increasing of pH value from 6.0 to 7.5 (see Fig. 3). After that, the fluorescence intensity decreased slowly. The same tendency can also be seen for the fluorescence intensity of $QDs_{(R)}$ at 590 nm which increases with the increasing of pH value from 6.5 to 7.5, though the increasing extent of fluorescence intensity of $QDs_{(R)}$ is less than that of $QDs_{(G)}$. It indicated that the pH has influence on the energy transfer between $QDs_{(G)}$ and $QDs_{(R)}$ to some extent. What is more, it can also influence the interaction between $QDs_{(G)}$ and immunoglobulin G. This result is consistent with the previous findings that the interaction between proteins and QDs is charge–charge electrostatic attraction [8].

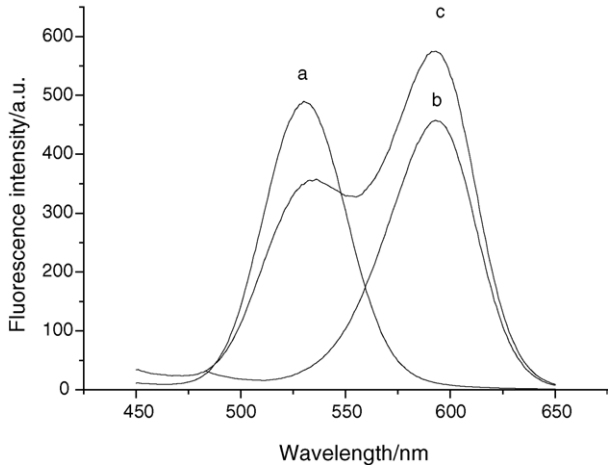

Fig. 2. Fluorescence spectra of $QDs_{(G)}$ labeled mouse IgG (a), $QDs_{(R)}$ labeled mouse IgG (b) and $QDs_{(G)}$–mouse IgG–$QDs_{(R)}$ (c). Excitation wavelength is 342 nm.

Considering that when the pH value of the PBS buffer solution was lower than 6.5, the QDs can be unstable in the aqueous environment and the protein was prone to denaturalization when the pH value was too high. Therefore, a pH of 7.3 was chosen in this study.

3.2.2. Effect of the ionic strength

It is well-known that the conjugation via electrostatic interaction is not stable enough and can be easily affected by ambient conditions, not only pH value but also ionic strength [25]. In above-mentioned studies, the analysis was carried out in a low concentration PBS buffer solution (2 mmol/L) with low ionic strength. To examine the influence of higher ionic strength on the interaction between QDs and immunoglobulin G, the fluorescence spectra of and $QDs_{(G)}$–IgG–$QDs_{(R)}$

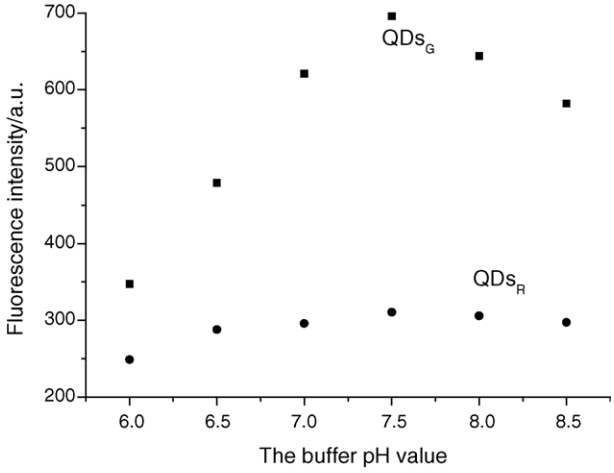

Fig. 3. The effect of the buffer pH value on the related fluorescence intensity of $QDs_{(G)}$ (square) and $QDs_{(R)}$ (circle) in $QDs_{(G)}$–mouse IgG–$QDs_{(R)}$ system.

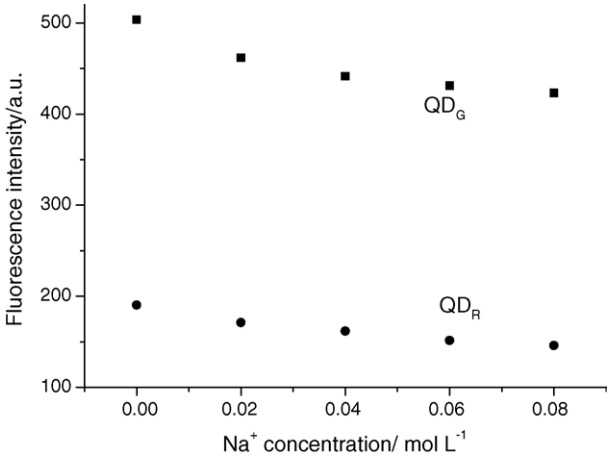

Fig. 4. The effect of ionic strength on the relative fluorescence intensity of $QDs_{(G)}$ (square) and $QDs_{(R)}$ (circle) in $QDs_{(G)}$–mouse IgG–$QDs_{(R)}$ system. A series of different volume of 0.5 mol/L NaCl solutions are added to the sample of CdTe and CdTe-ATR conjugates. Each salt concentration is calculated according to the resulting solution.

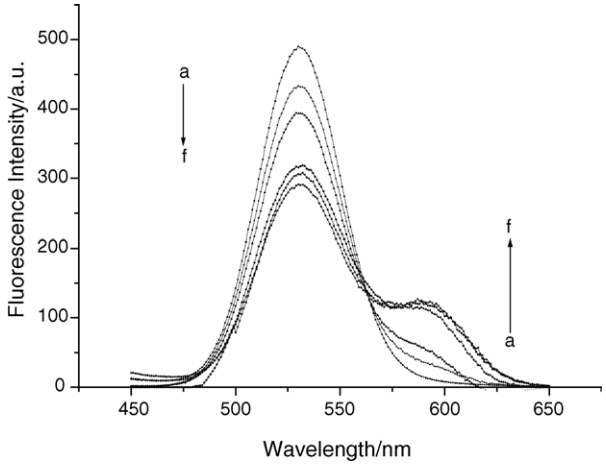

Fig. 5. Fluorescence emission spectra from solutions containing 0.05 mmol/L $QDs_{(G)}$, 4.0 mg/L mouse IgG and different concentration of $QDs_{(R)}$ solutions: (a) 0 mmol/L; (b) 0.025 mmol/l; (c) 0.05 mmol/L; (d) 0.1 mmol/L; (e) 0.125 mmol/L; (f) 0.187 mmol/L. All solutions were prepared in 2 mmol/L PBS buffer (pH 7.3). An excitation wavelength of 342 nm was used for all samples. The enhanced $QDs_{(R)}$ fluorescence intensity at 590 nm from the $QDs_{(G)}$–immunoglobulin–$QDs_{(R)}$ solutions as a function of $QDs_{(R)}$ concentration were obtained by extracting the $QDs_{(R)}$ fluorescence spectrum from each spectrum and correcting for background and direct $QDs_{(R)}$ excitation as described in the text.

solution were recorded as a function of increased NaCl concentration. It indicated that the ionic strength has a great effect on the binding in $QDs_{(G)}$–IgG–$QDs_{(R)}$ system. The fluorescence intensity at 535 and 590 nm were all decreased gradually along with the increasing of ionic strength (see Fig. 4), whereas the fluorescence intensity of free CdTe QDs shows no change upon salt addition as proved in our previous paper [26]. This phenomenon is a result of the counter-ion screening effect, which reduces the binding affinity of QDs to immunoglobulin. It was also confirmed that interaction between the QDs and protein is electrostatic binding.

3.3. Energy transfer between two sizes of CdTe QDs

In this work, the change of fluorescence spectra of $QDs_{(G)}$–IgG–$QDs_{(R)}$ solutions with gradually increasing quantity of $QDs_{(R)}$ to a fixed amount of $QDs_{(G)}$–IgG was studied. To see the change of the spectra clearly, the fluorescence intensities of $QDs_{(G)}$–IgG–$QDs_{(R)}$ solutions at 590 nm were obtained by extracting (obtained by fitting the region of the $QDs_{(R)}$ emission to a pure $QDs_{(R)}$ spectrum and then subtracting the fitted spectrum from the entire $QDs_{(G)}$–IgG–$QDs_{(R)}$ spectrum) the $QDs_{(R)}$ fluorescence spectrum from each spectrum and correcting for background and direct $QDs_{(R)}$ excitation (see Fig. 5). As expected, a significant enhancement of $QDs_{(R)}$ fluorescence intensity at 590 nm and the corresponding quenching of the green emission of $QDs_{(G)}$ at 535 nm are observed after the conjugation with mouse immunoglobulin G as the bridge. The enhancement in the $QDs_{(R)}$ fluorescence observed for the $QDs_{(G)}$–IgG–$QDs_{(R)}$ solutions indicates that a FRET process occurs between CdTe $QDs_{(G)}$ and $QDs_{(R)}$ due to the electrostatic attraction between negatively charged CdTe quantum dots and positively charged protein [8].

Quenching processes can be quantitatively described by the Stern–Volmer equation:

$$\frac{I_0}{I} = 1 + K_{sv}\,[\text{acceptor}] \tag{1}$$

where I is the integrated fluorescence intensity of the donor in the presence of the acceptor and I_0 the integrated fluorescence intensity of the donor in the absence of the acceptor [27]. K_{sv} is Stern–Volmer quenching constant. The FRET efficiency can be measured experimentally and is commonly defined as

$$E = 1 - \frac{I}{I_0} \tag{2}$$

The relation between energy transfer efficiency and the distance between the donor–acceptor pair is expressed as:

$$E = \frac{R_0^6}{R_0^6 + R^6} \tag{3}$$

where R_0 is the donor–acceptor distance at 50% energy transfer efficiency [28].

Fig. 5 shows that the $QD_{(G)}$ fluorescence intensity reduced rapidly with the increasing of $QDs_{(R)}$ concentration. In the range of $(0–1.25) \times 10^{-4}$ mol/L $QDs_{(R)}$, I_0/I increased linearly with the concentration of the $QDs_{(R)}$. By fitting the data with the Stern–Volmer equation, the Stern–Volmer constant was found to be 5.2×10^3 L/mol.

The FRET efficiency can also be measured when the concentration of $QDs_{(R)}$ was changed in the $QDs_{(G)}$–IgG–$QDs_{(R)}$ conjugation. When the concentration of $QDs_{(R)}$ exceeded 1.87×10^{-1} mmol/L, the $QDs_{(G)}$ fluorescence intensity did not change anymore. The FRET efficiency of

$QDs_{(G)}$–IgG–$QDs_{(R)}$ conjugation can reach to 40.59%. The R_0 for the $QDs_{(G)}$–IgG–$QDs_{(R)}$ donor–acceptor pair based on spectral overlap is 6.48 nm, by fitting the data with Eq. (3), the distance between the donor–acceptor was found to be 6.90 nm. These results confirm also that a FRET process occurs between $QDs_{(G)}$ donors and the $QDs_{(R)}$ acceptors.

To determine the binding ratio of both QDs with IgG, the concentrations of QDs and IgG in the reaction mixture were determined by the related UV–vis absorption signals of the CdTe QDs and IgG. At this time, we are unable to determine the exact stoichiometry of the $QDs_{(G)}$–IgG–$QDs_{(R)}$ complexes formed. A rough calculation of the average number of IgG present per QD was estimated to be about 1–2. Unlike the case of QD-DNA conjugates [29], the attachment of a greater number of IgG units to CdTe did not occur, most likely due to the steric hindrances related to the difficulty with the accommodation of bulky protein units around relatively small QDs (2–3 nm).

As the concentrations of $QDs_{(G)}$ and $QDs_{(R)}$ were fixed, the relation between the concentration of mouse immunoglobulin G and the fluorescence intensity ratio of $I_{acceptor}/I_{donor}$ were also studied under the optimal conditions in this work. The results were shown in Fig. 6. The insert displays the fluorescence intensity ratio of 590–535 nm as a function of the concentration of mouse immunoglobulin G. It can be seen that the $I_{acceptor}/I_{donor}$ increases linearly with the concentration of mouse immunoglobulin G. The linear regression equation is as follows: $I_{acceptor}/I_{donor} = 0.476 + 0.0237C_{mouse\text{-}IgG}$ (μg/mL). The coefficients of correlation is above 0.999 ($n = 4$). The detection limits of analytical processes based on FRET to the mouse immunoglobulin G can be as low as 0.042 mg/L. And the linear dynamic range of mouse IgG is 0.1–20.0 mg/L. From the dynamic ranges and detection limits for IgG, it is very clear that this method is sensitive.

3.4. Effect of papain on the FRET process

Further evidence for the conjugation of QDs and IgG is provided by studying the influence of papain on the FRET process of $QDs_{(G)}$–papain–$QDs_{(R)}$ bioconjugate system. Papain, a nonspecific protease, can digest of mouse IgG antibody (by cleaving mAb preferentially in the hinge region) [30]. In this work, papain solution was added to the bioconjugate solution, the results were showed in Fig. 7. It can be seen that, with the addition of papain, the fluorescence emission intensity of green-emitting QDs increases, and that of red-emitting QDs decreases synchronously. The FRET process of the bioconjugation system of IgG with two sizes CdTe QDs was prohibited. With the addition of papain, the quantity of mouse IgG bound to QDs reduced, which prohibits the FRET process. As a result, an increase of the green

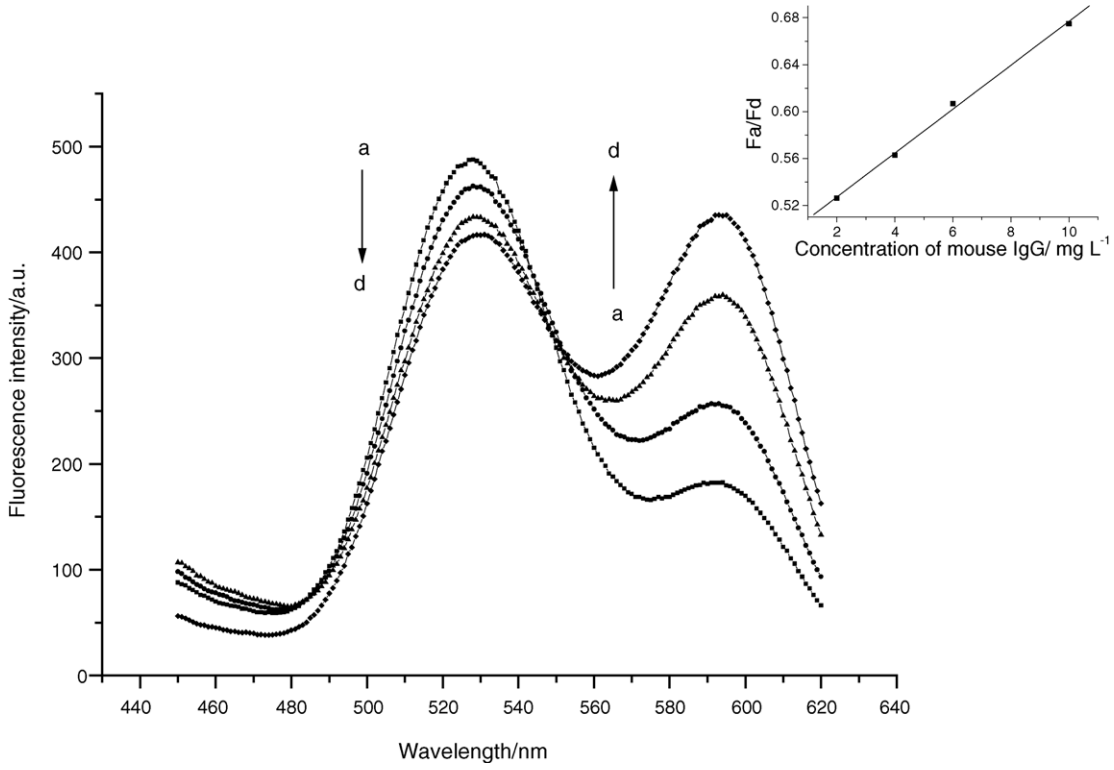

Fig. 6. Fluorescence emission spectra at a series of different concentration of mouse IgG labeled with same quantity of $QDs_{(G)}$ and $QDs_{(R)}$: (a) 2 mg/L; (b) 4 mg/L; (c) 6 mg/L; (d) 8 mg/L; (e) 10 mg/L mouse IgG. The insert displays the fluorescence intensity ratio of 590–535 nm as a function of the concentration of mouse immunoglobulin G.

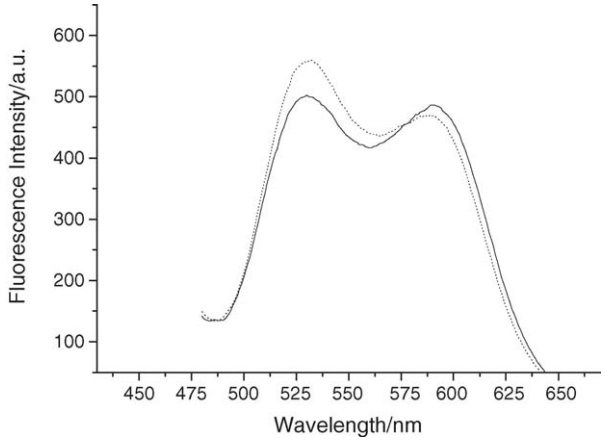

Fig. 7. Fluorescence spectra of the $QDs_{(G)}$–IgG–$QDs_{(R)}$ bioconjugate system without papain (solid) and with papain (dashed).

emission peak of QDs is observed again, while the red emission peak intensity decreases. This phenomenon can also prove that the dots are actually intimately associated with the IgG.

4. Conclusions

In summary, we have shown a FRET process between QDs of different sizes with the mouse immunoglobulin G as the binding bridge which results in an enhancement of fluorescence of the $QDs_{(R)}$ and a decline of that of the $QDs_{(G)}$. The two sizes of QDs can be used as probes for sensitive determination of protein with the advantage of simplicity, rapidity and practicability. We believe that with the further studies in this field, the donor–acceptor pair of QDs will be found more utilities and features in design of assays of antibody–antigen binding, DNA hybridization, and enzyme–substrate interaction, etc.

Acknowledgements

This work was financially supported by the National Natural Science Foundation of China (Project No. 20075009 and No. 20475020). The authors thank Prof. Shuming Nie (Wallace H. Coulter Department of Biomedical Engineering, Emory University and Georgia Institute of Technology) for the helpful suggestions.

References

[1] Q.H. Lowry, N.J. Rosebrough, A.L. Farr, R.J. Randall, J. Biol. Chem. 193 (1951) 265.
[2] M.M. Bradford, Anal. Biochem. 72 (1976) 163.
[3] R. Floresi, Anal. Biochem. 88 (1978) 605.
[4] K. Jung, E. Nickel, M. Pergande, Clin. Chim. Acta 187 (1990) 163.
[5] B.T. Doumas, W.A. Watson, H.G. Biggs, Clin. Chim. Acta 31 (1971) 87.
[6] M. Bruchez Jr, M. Moronne, P. Gin, S. Weiss, A.P. Alivisatos, Science 281 (1998) 2013.
[7] W.C.W. Chan, S. Nie, Science 281 (1998) 2016.
[8] H. Mattoussi, J.M. Mauro, E.R. Goldman, G.P. Anderson, V.C. Sundar, F.V. Mikulec, M.G. Bawendi, J. Am. Chem. Soc. 122 (2000) 12142.
[9] H. Mattoussi, J.M. Mauro, E.R. Goldman, T.M. Green, G.P. Anderson, V.C. Sundar, M.G. Bawendi, Phys. Stat. Sol. (b) 224 (2001) 277.
[10] L.Y. Wang, X.W. Kan, M.C. Zhang, C.Q. Zhu, L. Wang, Analyst 127 (2002) 1531.
[11] S.P. Wang, N. Mamedova, N.A. Kotov, W. Chen, J. Studer, Nano Lett. 2 (2002) 817.
[12] D.M. Wllard, L.L. Carillo, J. Jung, A.V. Orden, Nano Lett. 1 (2001) 469.
[13] P.T. Tran, E.R. Goldman, G.P. Anderson, J.M. Mauro, H. Mattoussi, Phys. Stat. Sol. 229 (2003) 1427.
[14] R.H. Fairclough, C.H. Cantor, Meth. Enzymol. 48 (1978) 347.
[15] P. Wu, L. Brand, Anal. Biochem. 218 (1994) 1.
[16] B.W. Van, D. Meer, G. Coker, S.Y. Chen, Resonance Energy Transfer: Theory and Data, VCH, New York, 1994.
[17] P.R. Selvin, Meth. Enzymol 246 (1995) 300.
[18] C.R. Kagan, C.B. Murray, M. Nirmal, M.G. Bawend, Phys. Rev. Lett. 76 (1996) 1517.
[19] C.R. Kagan, C.B. Murray, M.G. Bawendi, Phys. Rev. B 54 (1996) 8633.
[20] C.E. Finlayson, D.S. Ginger, N.C. Greenham, Chem. Phys. Lett. 338 (2001) 83.
[21] N.N. Mamedova, N.A. Kotov, A.L. Rogach, J. Studer, Nano Lett. 1 (2001) 281.
[22] M.Y. Gao, S. Kirstein, H. Möhwald, A.L. Rogach, A. Kornowski, A. Eychmüller, H. Weller, J. Phys. Chem. B 102 (1998) 8360.
[23] H. Zhang, Z. Zhou, B. Yang, M.Y. Gao, J. Phys. Chem. B 107 (2003) 8.
[24] J. Georges, N. Arnaud, L. Parise, Appl. Spectrosc. 50 (1996) 1505.
[25] Q.F. Li, S.H. Liu, H.Y. Zhang, X.G. Chen, Z.D. Hu, Anal. Lett. 34 (2001) 1133.
[26] Q.D. Chen, Z.B. Lin, X.G. Su, H. Zhang, X.H. He, B. Yang, Q.H. Jin, Int. J. Nanosci. 3 (2004) 273.
[27] A.R. Clapp, I.L. Medintz, J.M. Mauro, B.R. Fisher, M.G. Bawendi, H. Mattoussi, J. Am. Chem. Soc. 126 (2004) 301.
[28] J.R. Lakowicz, Principles of Florescence Spectroscopy, 2nd ed., Kluwer Academic/Plenum Press, New York, 1999.
[29] D. Zanchet, C.M. Micheel, W.J. Parak, D. Gerion, A.P. Alivisatos, Nano Lett. 1 (2001) 32.
[30] M. Adamczyk, J.C. Gebler, J. Wu, J. Immunol. Meth. 237 (2000) 95.